LBL-12767
c.2

Lawrence Berkeley Laboratory

UNIVERSITY OF CALIFORNIA

ENERGY & ENVIRONMENT DIVISION

RECEIVED
LAWRENCE BERKELEY LABORATORY
JUN 17
LIBRARY
DOCUMENTS

To be presented at the American Society of Mechanical Engineers 20th National Heat Transfer Conference, Milwaukee, WI, August 2-5, 1981

SOOT VOLUME FRACTION PROFILES IN A FREE COMBUSTING BOUNDARY LAYER

R.A. Beier and P.J. Pagni

May 1981

TWO-WEEK LOAN COPY

This is a Library Circulating Copy which may be borrowed for two weeks. For a personal retention copy, call Tech. Info. Division, Ext. 6782

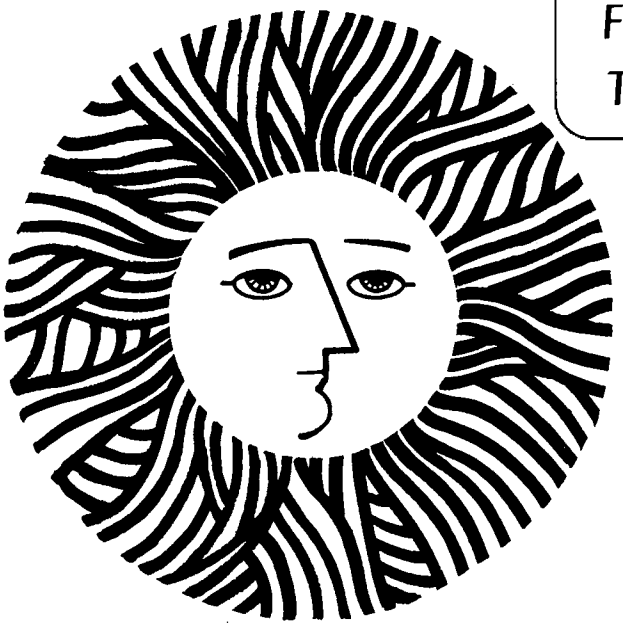

LBL-12767
c.2

Prepared for the U.S. Department of Energy under Contract W-7405-ENG-48

DISCLAIMER

This document was prepared as an account of work sponsored by the United States Government. While this document is believed to contain correct information, neither the United States Government nor any agency thereof, nor the Regents of the University of California, nor any of their employees, makes any warranty, express or implied, or assumes any legal responsibility for the accuracy, completeness, or usefulness of any information, apparatus, product, or process disclosed, or represents that its use would not infringe privately owned rights. Reference herein to any specific commercial product, process, or service by its trade name, trademark, manufacturer, or otherwise, does not necessarily constitute or imply its endorsement, recommendation, or favoring by the United States Government or any agency thereof, or the Regents of the University of California. The views and opinions of authors expressed herein do not necessarily state or reflect those of the United States Government or any agency thereof or the Regents of the University of California.

LBL-12767

SOOT VOLUME FRACTION PROFILES IN A FREE COMBUSTING BOUNDARY LAYER

R.A. Beier and P.J. Pagni
Mechancial Engineering Department

and

Lawrence Berkeley Laboratory
University of California
Berkeley, CA. 94720

This work was supported by the Center for Fire Research of the U.S.D.O.C. National Bureau of Standards under Grant No. NB 80 NAG-E6839 which was administered by the U.S. Department of Energy under Contract No. W-7405-ENG-48.

This manuscript was printed from originals provided by the authors.

ABSTRACT

Carbon particulate volume fraction profiles and approximate particle size distributions are measured in a free laminar combusting boundary layer for several liquid hydrocarbon fuels and PMMA (polymethylmethacrylate). A multiwavelength laser transmission technique determines a most probable particle radius and a total particle concentration, which are the two unknown parameters in an assumed Gauss size distribution. In the combusting boundary layer, a sooting region exists between the pyrolyzing fuel surface and the flame. The liquid fuel soot volume fractions range from $f_v \sim 10^{-7}$ for n-heptane, a paraffin, to $f_v \sim 10^{-5}$ for toluene, an aromatic. The PMMA soot volume fractions, $f_v \sim 5 \times 10^{-7}$, are approximately the same as the values previously reported for pool fires. The soot volume fractions increase slightly with downstream distance, while the standoff distance of the maximum in the f_v profile appears to approach the converging streamline. Convection of carbon particles broadens the soot region downstream. For all fuels tested, a most probable radius between 20 nm and 50 nm is obtained which varies only slightly with distance both downstream or normal to the fuel surface.

Table 1. Summary of fuel properties, sample geometries and peak soot volume fractions and size distributions

Fuel	B^a	$r_p{}^a$	$D_c{}^a$	Sample Width (cm)	Wave-length pair, i-j[b]	$(I/I_o)_i$	$(I/I_o)_j$	$f_v \times 10^6$	r_{max} (nm)	$N_o \times 10^{-9}$ (cm^{-3})
Liquids										
Toluene (C_7H_8)	5.5	0.09	26	3	1-4	0.0043	0.028	10	44	6.3
				3	2-4	0.0012	0.0096	13	45	7.2
Cyclohexene (C_6H_{10})	5.9	0.08	36	7	1-4	0.039	0.17	2.1	32	3.5
				7	2-4	0.10	0.25	1.9	31	3.5
Iso-octane (C_8H_{18})	6.3	0.08	28	3	1-4	0.52	0.69	1.0	36	1.2
				7	1-4	0.21	0.46	1.3	25	4.5
				15	1-4	0.063	0.24	1.1	27	3.0
				15	2-4	0.088	0.23	1.0	31	1.8
				15	3-4	0.11	0.23	1.1	27	3.0
Cyclohexane (C_6H_{12})	6.1	0.08	37	7	1-4	0.37	0.58	0.70	33	1.1
				15	1-4	0.15	0.35	0.67	32	1.1
n-Heptane (C_7H_{16})	5.6	0.08	29	7	1-4	0.54	0.73	0.43	28	1.0
				15	1-4	0.27	0.51	0.49	27	1.3
				15	2-4	0.39	0.55	0.36	35	0.46
Solid										
Polymethyl-methacrylate ($(C_5H_8O_2)_n$)	1.5	0.22	5.1	16	1-4	0.38	0.63	0.39	23	1.7

[a] Calculated from properties listed in Perry (25), Obert (26), and Varaftik (27) for all liquid fuels and from properties listed in Tewarson (28,29) for PMMA.

[b] i refers to λ_i as listed in the caption of Fig. 4.

INTRODUCTION

In most building fires thermal radiation is the dominant mode of heat transfer. Carbon particles within the flame are responsible for most of this emitted radiation and hence warrant quantification. Since a small, burning, vertical wall provides a two dimensional combusting boundary layer, which has been previously modeled (1-3), this fire is chosen for study. The volume fractions and size distributions of the soot particulate are determined using a multiwavelength laser transmission technique (4-8). In a steady, laminar, combusting boundary layer a pyrolysis zone separates a flame zone from the fuel surface as shown in Fig. 1. A layer on the fuel rich side of the blue flame zone is yellow, which indicates the presence of carbon particles. The width of the yellow soot layer increases with height. These measurements determine the soot volume fraction at different locations within the combusting layer for five liquid hydrocarbon fuels and one solid fuel as listed in Table 1.

Minchin (9) and Clarke, Hunter, and Garner (10) did early studies of the effect of fuel type on soot formation in laminar diffusion flames. They increased the height of a flame on a small, circular burner by increasing the fuel flow rate until the flame emitted soot at its tip. This height is callled the smoke height or smoke point. For comparing different fuels, a lower smoke point indicates a greater amount of soot formation. Recently, Glassman and Yaccarino (11) measured smoke points to show the importance of flame temperature in addition to fuel structure. The results

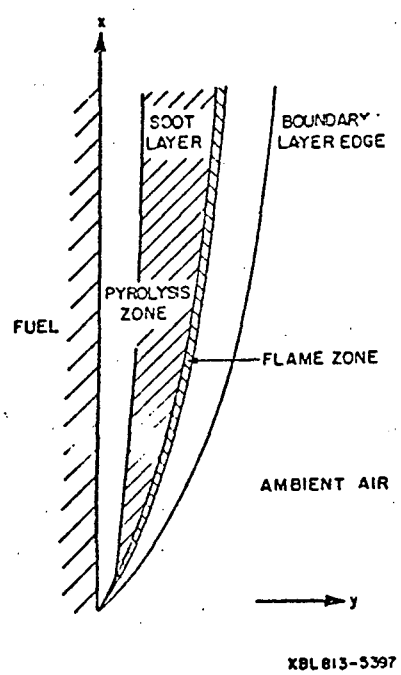

Fig. 1 Schematic diagram of a steady, two dimensional, free flow, laminar, combusting, boundary layer on a vertical pyrolyzing fuel slab.

of the present experiment quantify the effect of fuel type on the amount of soot produced by hydrocarbon fuels. These results also provide experimental bases for soot formation and destruction modeling by giving detailed profiles of soot volume fractions within a well characterized boundary layer.

Using a modified Schmidt Method technique, Markstein (12) determined absorption-emission coefficients and volume fraction of soot in pool fires. Pagni and Bard (4-8) measured the volume fraction of soot and particulate size distributions in pool fires. Jagoda, Prado, and Lahaye (13) measured local soot concentrations by probe and laser light scattering and absorption techniques in a candle-like diffusion flame. With these previous measurements, the results of the present study provide a comparison between soot volume fractions in a pool fire and a free flow boundary layer with the same fuel. Related experiments for gaseous fuels have been reported by Kent, Jander, and Wagner (14), and Haynes, Jander, and Wagner (15,16).

Sibulkin, Kulkarni, and Annamalai (17), Liu and Shih (18) and Kinoshita and Pagni (19) recently included radiation in models of a laminar combusting boundary layer. These models require a knowledge of the soot volume fraction within the layer, which is provided by the present study.

EXTINCTION ANALYSIS

The multiwavelength laser transmission technique is based on an extinction analysis, the details of which are described elsewhere (4-8), so only a brief outline of the analysis and assumptions is given here. The transmitted intensity, I, of a monochromatic beam through a polydisperse aerosol is related to the initial intensity, I_o by

$$I(\lambda)/I_o(\lambda) = \exp\,(-\tau(\lambda)L), \qquad (1)$$

where L is the beam pathlength. The aerosol spectral extinction coefficient, τ, is given by

$$\tau(\lambda,m,r) = \int_o^\infty N(r)\; Q(\lambda,m,r)\; \pi r^2 dr \qquad (2)$$

where Q is the particle extinction efficiency from the Mie scattering theory (20) for spherical particles. Calculation of the spectral extinction coefficient requires knowledge of the optical properties of soot, $m = n(1-ik)$, and the size distribution, N(r). The values of the optical properties used here were derived by Lee and Tien (21) partly based on data obtained by Bard and Pagni (5). A Gauss size distribution with $\sigma/r_m = 1/2$,

$$N(r)/N_o = (27\, r^3/2\, r^4_{max})\, \exp\,(-3\, r/r_{max}) \qquad (3)$$

is assumed, where r_{max} is the most probable radius, and N_o is the total particle concentration. The volume fraction of soot is defined by

$$f_v \equiv \frac{4}{3}\pi \int_o^\infty N(r)\; r^3 dr \qquad (4)$$

which, with equation (3), gives

$$f_v = \frac{54\pi}{3^8}\,\Gamma(7)\; N_o\; r^3_{max} = 18.62\; N_o\; r^3_{max} \qquad (5)$$

Measurements are made of the ratio of the transmitted and initial intensities, I/I_o, at two different wavelengths, superimposed over the same pathlength, L. Substituting these measured values into equation (1) gives two independent values of τ, one at each wavelength. These two τ values give two independent equations (2) to determine the two unknowns in the size distribution, N_o and r_{max} (4,5). The volume fraction of soot is simply obtained from equation (5).

Since soot particles may aglomerate in flows with long time scales, Lee and Tien (22) studied the effects of particle shape onthe radiative characteristics of a medium. From their calculations, considering spherical and cylindrical particles as limiting cases, particle shape is important in the far infrared region. For the visible wavelengths of these transmission measurements and the near infrared region of most flame radiation, calculations based on spherical particles give satisfactory results.

EXPERIMENTAL METHOD

The experimental setup, which is shown in Fig. 2, is similar to that described by Bard and Pagni (4-8). Two lasers are used: a Spectra-Physics Argon Ion

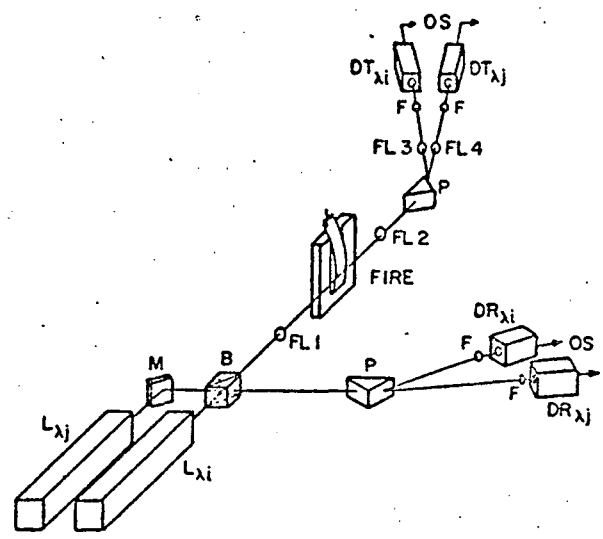

XBL813-5398

Fig. 2 Schematic diagram of apparatus for simultaneous multiwavelength laser transmission measurements.

$L_{\lambda i}$, $L_{\lambda j}$	- Laser at λ_i or λ_j
M	- Mirror
B	- Beamsplitter
P	- Prism
FL1	- Focusing lens #1 (f = 550 mm)
FL2	- Focusing lens #2 (f = 250 mm)
FL3	- Focusing lens #3 (f = 200 mm)
FL4	- Focusing lens #4 (f = 78 mm)
F	- Bandpass filter (bandwidth = 30 A)
$DT_{\lambda i}$, $DT_{\lambda j}$	- Detector for transmitted intensity
$DR_{\lambda i}$, $DR_{\lambda j}$	- Detector for reference intensity
OS	- Output signal to amplifier and computer

tunable laser model 165, operating at either $\lambda = 0.4579$ μm, 0.4880 μm, or 0.5145 μm, and a Spectra-Physics Helium Neon laser model 125, emitting at $\lambda = 0.6328$ μm. After a cube beam splitter superimposes the two beams from the lasers, the beams pass through the same physical space in the fire. A first simple lens reduces the diameter of the beams in the fire. After a second lens collects the transmitted light, an equilaterial prism separates the two beams. Each beam passes through another focusing lens and a narrow band pass filter, before it strikes a laser power meter (Newport Research Corp., model 820). The beam splitter provides a second beam from each laser, which is monitored as a reference intensity by the same prism-detector system. A PDP-11/34 microcomputer stores the data, after the output signals from the detector pass through a d.c. amplifier and a (Digital Equipment Corp.) AR11 16-channel, 10 bit, A/D converter. A digital timer, with an adjustable period, triggers the A/D converter to read the output signals of the detectors.

The liquid fueled wick and the solid fuel, are mounted in a small, vertical wall which is bolted to a milling table. The inert wall is made of Marinite-XL (Johns-Manville Co.), and its width and height are 0.5 m. The wick, ceramic fiber board (Fiberfrax Hot Board, Carborundum Co.), has its front surface flush with the inert wall surface. With aluminum foil around the hidden surfaces of the wick, the inert wall does not absorb liquid fuel.

Since the transmission of the laser beams varies greatly for the different fuels, wicks of different widths are used as listed in Table 1. The most frequently used wick sizes are 12 cm high and 15 cm or 7 cm wide. The samples of PMMA are 15 cm high, 16 cm wide, and 1.27 cm thick. The diameter of the laser beam in the flame limits the spatial resolution of the transmission measurement. For pathlengths of 16 cm and 7 cm the maximum beam width between points of $1/e^2$ intensity is less than 0.4 mm and 0.3 mm, respectively.

Since variations in temperature and species change the index of refraction in the direction normal to the fuel surface, the fire can deflect the laser beam. The angular deflection of the beam in the combusting boundary layer is greater than the deflection in pool fires (5-8), due to the steeper gradients of the species and temperature profiles in the boundary layer. This angular deflection changes the beam pathlengths in the prism and if uncorrected can cause the beams to miss the detectors. Lens FL2 in Fig. 2 is used to minimize the beam movement relative to the prism and thus to the detectors. The position of lens FL2 bisects the distance between the prism and the center of the fire, which is set at four times the focal length of lens FL2. This arrangement projects an image of the beam at the center of the fire onto the prism. The small movement of the beam at the center of the fire then gives only small movement at the prism.

The deflection of the beam in the fire is measured for all the fuels. For liquid fuels the deflection does not decrease the spatial resolution significantly except near the inner edge of the soot layer when the width of the wick is 15 cm. Therefore, data near the inner boundary of the soot layer are obtained from measurements with shorter pathlengths. Since the deflection of the beam is less for PMMA, a larger pathlength of 16 cm is used.

The distance between the superimposed laser beams and the fuel surface is changed by moving the fire horizontally. A complete scan of the fire is obtained by adjusting the height of the wall between traverses. After the fuel is ignited, a sheet of pyrex glass is placed in front of the fire about 0.25 m from the fuel surface to block disturbances from air movements in the room. For liquid fuels the supply of fuel in the wick gives a steady flame for about five minutes after a very short transient. This time period allows one horizontal scan, with increments of ∿ 0.4 mm, through the boundary layer each time the fire is ignited. At each position the outputs of the detectors are read 300 times within a 6 second interval. After each horizontal scan the fire is extinguished, the downstream location or height is changed by lowering the wall and the wick is soaked with fuel before the fire is reignited.

The pathlength, L, is approximately 1 cm longer than the wick width. It is measured by placing a scale in front of the flame at the laser beam location. End effects may be neglected for these large L. The measured values of I/I_o for the two different wavelengths and L are used in the extinction analysis to calculate r_{max} and f_v. Data for more than one wavelength pair may be used to isolate the correct value of r_{max} (4-8).

For PMMA the fuel regression rate affects the beam distance from the fuel surface. The regression rate is measured in a similar experiment by blocking the laser beams partially with the fuel surface. If the vertical wall remains stationary, the surface of the pyrolyzing fuel slab recedes and blocks a smaller part of the laser beams. The regression rate is given by the rate of the vertical wall has to be moved to maintain a constant reading of transmitted intensity for the partially blocked beam. The regression rate was measured before and after each horizontal scan through the boundary layer. A new sample of PMMA is burned for the transmission measurements at each height.

Due to some unsteadiness in the fire, the positions of the soot layer and the flame zone fluctuate. Near the boundaries of the soot zone, a point at a fixed distance from the fuel surface spends only part of the time in the soot layer. Likewise, only a part of the pathlength of the laser beam may be in the soot layer at any time. Since the measured pathlength is the entire width of the fire, transmission measurements near a boundary may give too high a value of I/I_o, and therefore, a lower volume fraction of soot than the true value. At the outer soot layer edge the portion of the beam in the soot layer is visible from light which is scattered by the soot. While the measurements are made, positions are noted where only a fraction of the beam is in the soot layer. At the inner boundary an increase in the experimental standard deviations of the volume fraction of soot and the most probable radius occurs. On these bases data points are rejected where $\sigma_{fv}/f_v > 0.4$. The increase in the error bars in Figs. 3-6 at the soot layer boundaries is largely due to these fluctuations.

RESULTS AND DISCUSSION

Profiles of the volume fraction of soot are shown in Fig. 3 for five liquid fuels and PMMA at a height of 4 cm above the leading edge of the fuel surface. Results from at least two different horizontal scans are shown for each fuel. Limitations on reproducing the same fire account for most of the scatter in the data. Table 1 lists values of soot volume fractions, the most probable radius, and total particle concentrations at the peaks of these profiles. Since no signi-

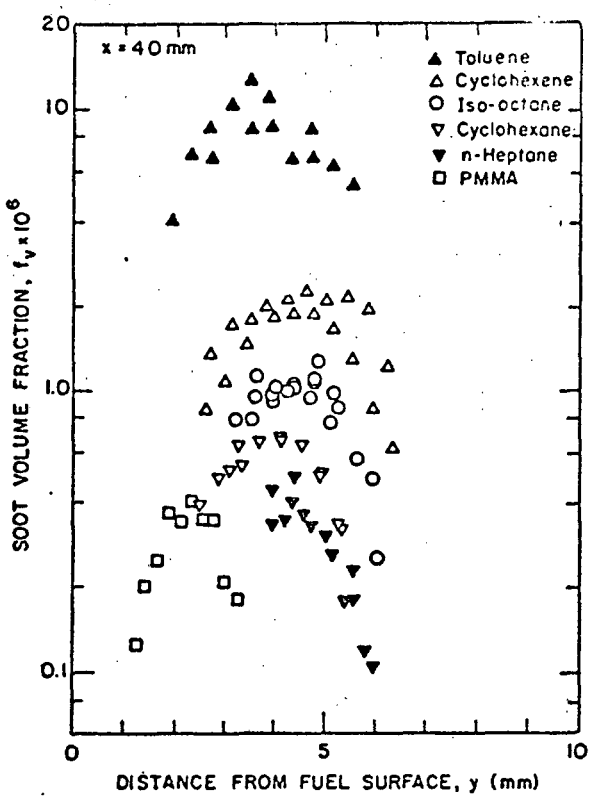

XBL 813-5399

Fig. 3 Soot volume fractions, f_v, as a function of distance from fuel surface at a height of 40 mm for five liquid hydrocarbon fuels and PMMA.

ficant change in the data occurs for wicks of different widths, errors due to the end effects are negligible. The volume fraction of soot for toluene, an aromatic

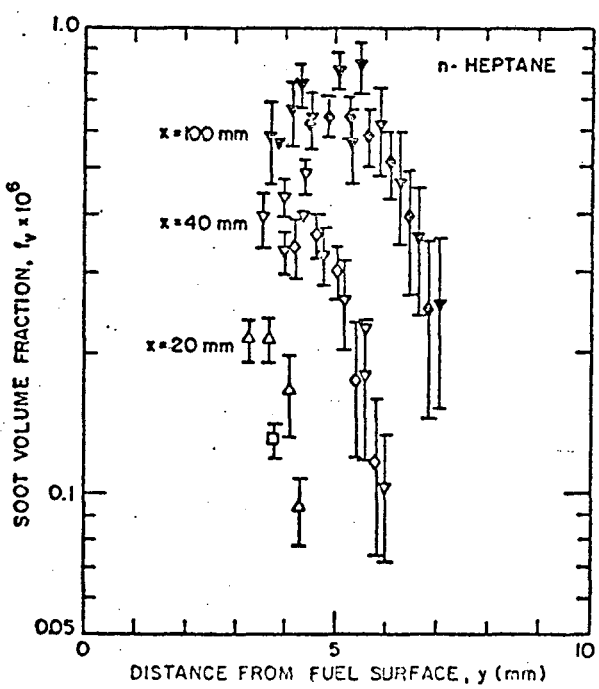

XBL 813-5400

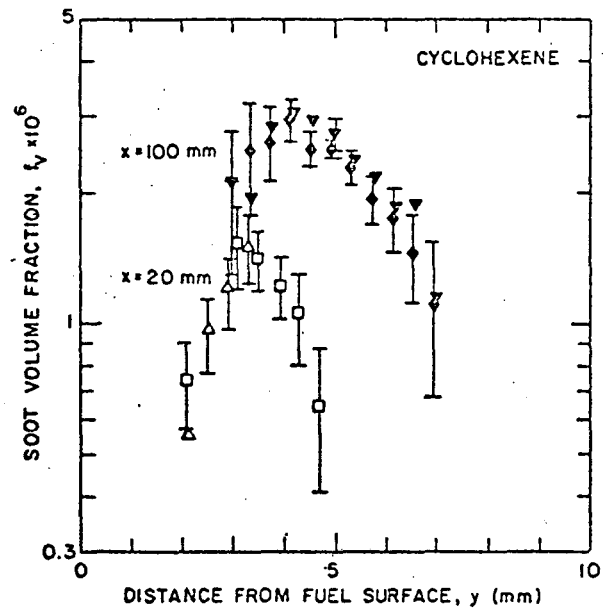

XBL 813-5401

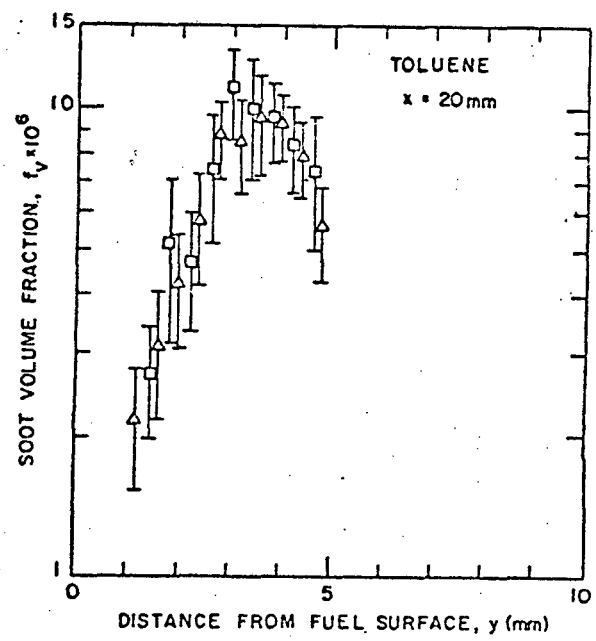

XBL 813-5402

Fig. 4 Soot volume fractions, f_v, as a function of distance from fuel surface at different heights for a) n-heptane; b) cyclohexene; c) toluene. Wavelength pair numbers refer to λ_1 (λ_1 = 0.4579 μm, λ_2 = 0.4880 μm, λ_3 = 0.5145 μm, λ_4 = 0.6328 μm).

Symbol	x (mm)	Wavelength Pair
△	20	1-4
□	20	2-4
▽	40	1-4
◇	40	2-4
▼	100	1-4
◆	100	2-4

compound, is exceptionally large. Previous studies of soot formation have found that aromatics have an unusually large sooting tendency (23). The five liquid fuels were included in tests for smoke points by Clarke, Hunter, and Garner (10). Their ranking of the fuels for the amount of soot formation agrees with the data in Fig. 3.

Previous measurements in small pool fires (4-8,24) show the volume fraction of soot at 2 cm above the fuel surface for PMMA, iso-octane, and toluene are 0.22×10^{-6}, 0.46×10^{-6}, and 4.8×10^{-6}, respectively. The pool fire results are average values across the fire; it is interesting that they lie between the maximum and minimum values of the profiles found here in free boundary layers.

Figures 4a, b, and c present profiles of the volume fraction of soot at various heights above the leading edge of the fuel surface for n-heptane, cyclohexene, and toluene. Experimental standard deviations of f_v are shown by the error bars, which were obtained from standard deviations in the extinction coefficients by standard statistical techniques (7). Error bars are omitted where they would mask trends. The increase in the soot volume fraction for n-heptane is large between the heights of 2 cm and 4 cm, but the amount of increase diminishes with height. Unlike the results for n-heptane, the maximum soot volume fraction for toluene does not change significantly between the heights of 2 cm and 4 cm (compare Figs. 3 and 4c). The variation of soot volume fraction with height for cyclohexene falls between the two limiting cases of n-heptane and toluene. As the height increases the outer edge of the soot layer follows the blue flame zone away from the fuel surface, and the width of the soot layer increases. At the lower heights the effects due to the opposing processes of formation and oxidation of soot are more apparent, causing sharply peaked f_v profiles. Figures 4a and c show that soot particulate is found closer to the fuel surface for toluene than for n-heptane at a height of 2 cm. It is unclear if soot particles are formed closer to the wall for toluene, because convection from the higher concentration of soot particles upstream widens the soot layer. The shape of the profile for cyclohexene at a height of 2 cm falls between the two limiting liquid-fueled cases of n-heptane and toluene. Although the position of the inner edge of the soot layer varies among fuels, the location of the outer edge is approximately the same for all the liquid fuels. Since the thermophysical properties of these hydrocarbon fuels are similar, as shown in Table 1, the location of the flame zone is approximately the same. The peak of the profile shifts toward the fuel surface relative to the edges of the soot layer with increasing height for cyclohexene and toluene, while the opposite trend is observed for the less soot flames.

In Fig. 5 the profiles of soot volume fraction for PMMA are shown at heights of 4 cm and 10 cm above the leading edge of the fuel surface. The maximum in the profile increases only slightly with height. The distance of the flame zone from the fuel surface is less for PMMA than the liquid fuels, and the distance between the peak of the profile and the fuel surface remains approximately constant with height above 4 cm.

For all the fuels the most probable radius, r_{max}, is between 20 nm and 50 nm, and the particle radii do not change significantly across the soot layer. Fig. 6 presents profiles of r_{max} at 2 cm and 10 cm above the leading edge for cyclohexene. The slight increase of r_{max} with height is typical for the fuels in this study. Similar results have been obtained in pool fires (4-8).

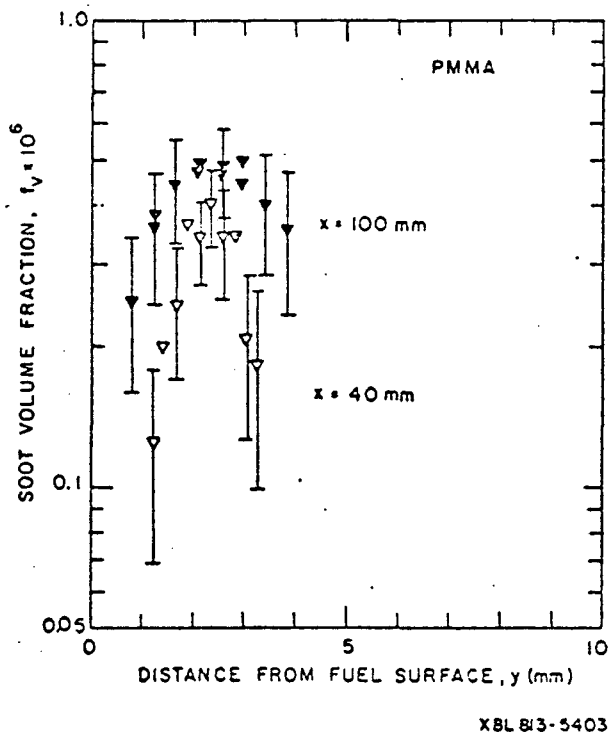

Fig. 5 Soot volume fractions, f_v, for PMMA as a function of distance from the fuel surface. The symbol definitions are those given in the caption to Fig. 4.

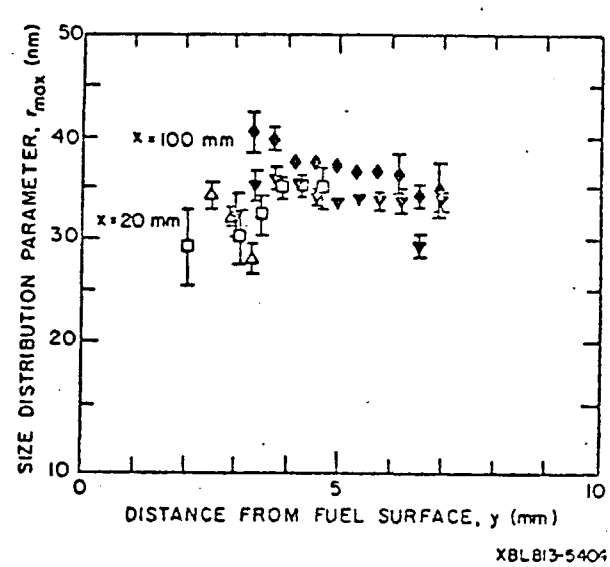

Fig. 6 Most probable particle radius, r_{max}, as a function of distance from the fuel surface and downstream for cyclohexene. The symbol definitions are those given in the caption to Fig. 4.

CONCLUSIONS

Soot volume fractions and size distributions have been measured in a well characterized combusting boundary layer in free flow for five liquid fuels and PMMA. A soot region is observed at the fuel side of the flame front. The ranking of fuels by soot volume fraction is preserved between small pool fires and the free laminar combusting boundary layer. A previous ranking of the fuels by their smoke point also agrees with these measurements of soot volume fractions. In the laminar boundary layer the soot volume fraction increases with downstream distance for all fuels, but for fuels with a high soot volume fraction the variation is small. When the width of the soot layer is compared for different liquid fuels near the leading edge, a more sooty fuel produces a wider soot layer; e.g. for n-heptane the soot region is observed to be quite narrow. The convection of particles downstream widens the soot layer until, at a height of $\sim$ 10 cm above the fuel leading edge, the width of the soot layer is approximately constant for all the liquid fuels. The particle radii increase only very slightly with downstream distances for all the fuels tested.

In the future, the well characterized nature of this radiating, combusting boundary layer will permit analyses of the effects of the soot particulates of the complex interaction among: convection due to buoyant flow and thermophoretic forces, Brownian diffussion, formation, surface growth, and oxidation. Additional experiments are planned in forced flow boundary layers with a wide range of free stream oxygen concentrations. These data, along with computations of the velocity, species, and thermal field provide bases for soot formation modeling.

ACKNOWLEDGEMENTS

This work was supported by the Center for Fire Research of the National Bureau of Standards, U.S. Department of Commerce.

REFERENCES

1 Kim, J.S., deRis, J., and Kroesser, F.W., "Laminar Free-Convective Burning of Fuel Surface," Thirteenth Symposium (International) on Combusting, pp. 949-961, The Combustion Institute, 1971.

2 Kosdon, F.J., Williams, F.A., and Buman, C., "Combustion of Vertical Cellulosic Cylinders in Air," Twelfth Symposium (International) on Combustion, pp. 253-264, The Combustion Institute, 1969.

3 Pagni, P.J., and Shih, T.M., "Excess Pyrolyzate," Sixteenth Symposium (International) on Combustion, pp. 1329-1342, The Combustion Institute, 1976.

4 Pagni, P.J., and Bard, S., "Particulate Volume Fractions in Diffusion Flames," Seventeenth Symposium (International) on Combustion, pp. 1017-1028, The Combustion Institute, 1978.

5 Bard, S. and Pagni, P.J., "Carbon Particulate in Small Pool Fire Flames," ASME Journal of Heat Transfer, in press.

6 Bard, S. and Pagni, P.J., "Spatial Variation of Soot Volume Fractions in Pool Fire Diffusion Flames," Combustion and Flame, in preparation.

7 Bard, S., "Diffusion Flame Particulate Volume Fractions," Ph.D. Dissertation, Mechanical Engineering Department, University of California, Berkeley, 1980.

8 Bard, S., and Pagni, P.J., "Comparison of Laser Induced Flourescence and Scattering in Pool Fire Diffusion Flames," J. Quant. Spec. Rad. Trans., 25:5, 453-461, 1981.

9 Minchin, S.T., "Luminous Stationary Flames: the Quantitative Relationship between Flame Dimensions at the Sooting Point and Chemical Composition, with Special Reference to Petroleum Hydrocarbons," Journal of the Institute of Petroleum Technologists, Vol. 17, 1931, pp. 102-120.

10 Clarke, A.E., Hunter, T.G., and Garner, F.H., "The Tendency to Smoke of Organic Substances on Burning, Part I," Journal of the Institute of Petroleum Technologists, Vol. 32, May 1946, pp. 627-642.

11 Glassman, I., and Yaccarino, P., "The Temperature Effect in Sooting Diffusion Flames," Eighteenth Symposium (International) on Combustion, The Combustion Institute, 1980, in press.

12 Markstein, G.H., "Radiative Properties of Plastic Fires," Seventeen Symposium (International) on Combustion, pp. 1053-1062, Combustion Institute, 1978.

13 Jagoda, I.J., Prado, G., and Lahaye, J., "An Experimental Investigation into Soot Formation and Distribution in Polymer Diffusion Flames," Combustion and Flame, Vol. 37, 1980, pp. 261-274.

14 Kent, J.H., Jander, H., and Wagner, H.Gg., "Soot Formation in Laminar Diffusion Flame," Eighteenth Symposium (International) on Combustion, The Combustion Institute, 1980, in press.

15 Haynes, B.S., and Wagner, H.Gg., "Sooting Structure in a Laminar Diffusion Flame," Ber. Bunsenges. Phys. Chem., Vol. 84, 1980, pp. 499-506.

16 Haynes, B.S., Jander, H., and Wagner, H.Gg., "Optical Studies of Soot-Formation Processes in Premixed Flames," Ber. Bunsenges. Phys. Chem., Vol. 84, 1980, pp. 585-592.

17 Sibulkin, M., Kulkarni, A.K., Annamalai, K., "Effects of Radiation on the Burning of Vertical Fuel Surfaces," Eighteenth Symposium (International) on Combustion, Combustion Institute, 1980, in press.

18 Liu, C.N., and Shih, T.M., "Laminar, Mixed-Convection, Boundary-Layer, Nongray-Radiative, Diffusion Flames," ASME Journal of Heat Transfer, Vol. 102, 1980, pp. 724-730.

19 Kinoshita and Pagni, P.J., "Stagnation-Point Combustion with Radiation," Eighteenth Symposium (International) on Combustion, in press, The Combustion Institute, Pittsburgh, PA., 1981.

20 Kerker, M., The Scattering of Light and Other Electromagnetic Radiation, Academic Press, 1969.

21 Lee, S.C. and Tien, C.L., "Optical Constants of Soot in Hydrocarbon Flames," Eighteenth Symposium (International) on Combustion, Combustion Institute, 1980, in press.

22 Lee, S.C., and Tien, C.L., "Thermal Radiation of Spherical and Cylindrical Soot Particles," Paper No. 80-54, Western States Section of the Combustion Institute, Fall Meeting, 1980.

23 Bittner, J.D., and Howard, J.B., "Role of Aromatics in Soot Formation," in Alternative Hydrocarbon Fuels: Combustion and Chemical Kinetics, Vol. 62, Progress in Astronautics and Aeronautics, Amer. Inst. of Aero. and Astro., New York, pp. 335-358.

24 Lee, S.C., "Soot Radiation From Diffusion Flames," Ph.D. Dissertation, Mechancial Engineering Department, University of California, Berkeley, 1981.

25 Perry, J.H., Chemical Engineers' Handbook, McGraw-Hill, New York, 1975.

26 Obert, E.F., Internal Combustion Engines, International Textbook Co., Scranton, Penn., 1968.

27 Varaftik, N.B., Tables of Thermophysical Properties of Liquids and Gases, Hemisphere Publishing Corp., distributed by John Wiley, 1975.

28 Tewarson, A. and Pion, R.F., "A Laboratory-Scale Test Method for the Measurement of Flammability Parameters," Technical Report No. 22524, FMRC, Norwood, Mass., October 1977.

29 Tewarson, A., "Experimental Evaluation of Flammability Parameters of Polymetric Materials, Technical Report No. 22524, RC79-T9, FMRC, Norwood, Mass., February 1979.

NOMENCLATURE

B	mass transfer number, $(Q_p Y_{ox,\infty} - h_w)/L_p$
c_p	specific heat
D_c	dimensionless heat of combustion, $Q_p Y_{ox,\infty}/h_w$
h	specific enthalpy, $\int_{T_\infty}^{T} c_p \, dT$
f_v	particulate carbon volume/flame volume
I	radiant intensity
L	beam pathlength through fire
L_p	effective latent heat of pyrolysis
L_λ	laser at λ
m	complex index of refraction
M_i	molecular weight of species i
n	real index of refraction
nk	imaginary index of refraction
$N(r)dr$	particle concentration in the size range dr about r
N	total particle concentration
Q	extinction efficiency
Q_p	heat of reaction per unit mass of oxygen
r	particle radius
r_p	mass consumption number, $Y_{ox,\infty} \nu_f M_f / Y_{fw} \nu_{ox} M_{ox}$
T	temperature
Y_i	mass fraction of species i
Y_{fw}	wall fuel mass fraction, $[Y_{ft} B - Y_{ox,\infty} (\nu_f M_f / \nu_{ox} M_{ox})]/(1 + B)$
λ	wavelength
ν	stoichiometric coefficient
σ	standard deviation
τ	extinction coefficient

SUBSCRIPTS

f	fuel
ft	fuel in the transferred (pyrolyzed) material
i	first wavelength
j	second wavelength
max	most probable, i.e., at maximum in N(r)
o	incident
ox	oxidizer
w	fuel surface
∞	ambient

This report was done with support from the Department of Energy. Any conclusions or opinions expressed in this report represent solely those of the author(s) and not necessarily those of The Regents of the University of California, the Lawrence Berkeley Laboratory or the Department of Energy.

Reference to a company or product name does not imply approval or recommendation of the product by the University of California or the U.S. Department of Energy to the exclusion of others that may be suitable.

TECHNICAL INFORMATION DEPARTMENT
LAWRENCE BERKELEY LABORATORY
UNIVERSITY OF CALIFORNIA
BERKELEY, CALIFORNIA 94720